European Journal of Agronomy 154 (2024) 127075

Contents lists available at ScienceDirect

European Journal of Agronomy

journal homepage: www.elsevier.com/locate/eja

Adapting the grassland model BASGRA to simulate yield and nutritive value of whole-crop barley

Tomas Persson [a,*], Mats Höglind [a], Johanna Wallsten [b], Elisabet Nadeau [c,e], Xiao Huang [a,1], Bengt-Ove Rustas [d]

[a] Norwegian Institute of Bioeconomy Research (NIBIO), P.O Box 115, NO-1431 Ås, Norway
[b] Department of Crop Production Ecology, Swedish University of Agricultural Sciences, 901 83 Umeå, Sweden
[c] Department of Animal Environment and Health, Swedish University of Agricultural Sciences, Box 234, 532 23 Skara, Sweden
[d] Department of Animal Nutrition and Management, Swedish University of Agricultural Sciences, Box 7024, 750 07 Uppsala, Sweden
[e] Rural Economy and Agricultural Society Sjuhärad, Box 5007, 514 05 Länghem, Sweden

ARTICLE INFO

Keywords:
Climate change
Crude protein
Digestibility
Fibre
Process-based model
Silage

ABSTRACT

Ensiling of whole-crop biomass of barley before full maturity is common practice in regions with a short growing season. The developmental stage of barley at harvest can have a large impact on yield and nutritive composition. The relationships between crop growth, environmental conditions and crop management can be described in process-based simulation models. Some models, including the Basic Grassland (BASGRA) model, have been developed to simulate the yield and nutritive value of forage grasses, and usually evaluated against metrics of relevance for whole-crop silage. The objectives of this study were to: i) modify the BASGRA model to simulate whole-crop spring barley; ii) evaluate the performance of this model against empirical data on dry matter (DM) yield and nutritive value attributes from field experiments, divided into geographical regions; and iii) evaluate DM yield, nutritive value and cutting date under current and future climate conditions for three locations in Sweden and four cutting regimes. Main model modifications included addition of a spike pool, equations for carbon (C) and nitrogen (N) allocation to the spike pool and equations for C and N translocation from vegetative plant parts to spikes. Model calibration and validation against field trial data from Sweden, including samples harvested from late anthesis stage to hard dough stage that were either pooled or divided into regions, showed better prediction accuracy, evaluated as normalised root mean squared error (RMSE), of neutral detergent fibre (NDF) (7.58–18.4%) than of DM yield (16.8–27.8%), crude protein (15.5–23.2%) or digestible organic matter in the DM (DOMD) (12.0–22.2%). Model prediction using weather data representing 1990–2020 and 2021–2040 climate conditions for three locations in Sweden (Skara, Umeå, Uppsala) showed lower DM yield, earlier harvest and slightly higher NDF concentration on average (across locations and developmental stage at cutting) when using near-future climate data rather than historical data. The model can be used to evaluate whole-crop barley performance under production conditions in Sweden or in other countries with similar climate, soils and crop management regimes.

1. Introduction

Ensiling the whole biomass fraction, including grain and vegetative fractions, of small-grain cereals before full maturity is a common forage conservation method in regions with a short growing season, such as northern Europe (Wallsten et al., 2010; Rustas et al., 2011; Huuskonen et al., 2017; Randby et al., 2019), or in regions where such crops can be grown during the winter season between two summer crops (Park et al., 2008; Xu et al., 2021). Small-grain cereals are also conserved as whole-crop silage in subtropical and tropical regions with rainy and dry seasons, such as southern Brazil (Leão et al., 2017; Bueno et al., 2018). The developmental stage of the whole crop at harvest can have a large impact on its dry matter (DM) yield and nutritive value (Crovetto et al., 1998; Rustas et al., 2010; Nadeau et al., 2019). The nutritive value, including energy content (Crovetto et al., 1998), sugar, fibre and protein content and fibre digestibility, generally decreases from the heading

---

* Corresponding author.
E-mail address: tomas.persson@nibio.no (T. Persson).

[1] Current address: College of Ecology and Environment, Collaborative Innovation Center of Ecological Civilization, Hainan University, 570100 Haikou, China

https://doi.org/10.1016/j.eja.2023.127075
Received 31 August 2023; Received in revised form 30 December 2023; Accepted 31 December 2023
Available online 8 January 2024
1161-0301/© 2024 The Author(s). Published by Elsevier B.V. This is an open access article under the CC BY license (http://creativecommons.org/licenses/by/4.0/).

stage to the dough stage, i.e. the period in which whole crops for ensiling are normally harvested, while the starch content increases (Nadeau, 2007; Wallsten and Hatfield, 2016; Randby et al., 2019). These changes coincide with changes in the ratio of grain to vegetative tissue biomass (grain/straw ratio) (AHDB, 2018) and physiological changes within vegetative and grain tissues (Seog et al., 1993; Khorasani et al., 1997; Gubatz and Shewry, 2010). These changes in nutrient composition in whole-crop barley result in different animal production responses. They also affect how the feed can be used in diets for ruminants differing in production intensity and physiological state (Nadeau, 2007), such as lactating and non-lactating cows.

Growth, development, biomass yield and nutritive composition of barley and other cereal crops are highly dependent on the prevailing weather and soil conditions, and on management practices such as sowing date and seed and fertiliser rate (Slafer et al., 2002). The relationships between these factors are described in different process-based models (Brisson et al., 2003; Jones et al., 2003; Holzworth et al., 2014; Stöckle et al., 2014), which can be used as decision support for farmers and farm advisors. Several crop simulation models have been applied to simulate phenological development, biomass and grain yield of spring and winter barley under different climate conditions (Rötter et al., 2012; Tao et al., 2020). To date, the main priority in barley and other cereal crop modelling studies has been to predict grain yield at full maturity. Less effort has been devoted to predicting aboveground biomass and its underlying components at earlier developmental stages. Moreover, cereal crop models generally do not simulate whole-crop nutritive attributes such as fibre content and digestibility, which are important characteristics. In contrast, there are forage grass models such as CATIMO (Bonesmo and Belanger, 2002b), STICS (Jégo et al., 2013) and the Basic Grassland model (BASGRA) (Höglind et al., 2020) that contain equations for fibre content and digestibility, as the nutritive value of forage grasses is often simulated due to their importance in ruminant feeding. The latter model has been developed primarily for northern European conditions. Its ability to simulate forage grass, including both biomass (Korhonen et al., 2018) and nutritive value attributes such as fibre and protein content and digestibility (Persson et al., 2019), has also been extensively evaluated for this region. Moreover, the BASGRA model includes modules for winter stresses and their effect on winter survival (Höglind et al., 2016), which are processes that are also relevant for winter cereals. In total, this makes BASGRA a suitable candidate to adapt for use in whole-crop cereal simulations. However, the prediction accuracy of both the LINGRA model (Persson et al., 2014), a predecessor to BASGRA, and cereal crop models (Hao et al., 2021) has varied between locations or depending on the geographic distribution of the data that were used for model calibration. Moreover, Angulo et al. (2013), in a study of different calibration approaches of process-based models for five crops in Europe, including winter wheat and winter barley, concluded that regional projections with crop models can be improved if they are calibrated with regional specific data. Therefore, a comparison of different geographical distributions of calibration data could possibly provide information that is useful for further model applications and development of BASGRA for whole-crop barley in northern Europe.

The objectives of this study were to: i) modify the BASGRA model to simulate whole-crop spring barley; ii) evaluate the performance of the modified model against empirical data on DM yield and nutritive value attributes obtained under controlled field experimental conditions; iii) evaluate the importance of the geographic distribution of the calibration data for the model performance; and iv) evaluate DM yield, nutritive value and cutting date under current and projected future climate conditions for three locations in Sweden and four cutting regimes.

2. Material and methods

2.1. Model adaption

The BASGRA model, which was originally developed to simulate DM yield (Höglind et al., 2001; Höglind et al., 2016), crude protein, fibre content and digestibility (Höglind et al., 2020) of the forage grass timothy, was adapted to simulate these four variables for whole-crop barley as a function of weather, soil and crop management. In the forage grass version of BASGRA, plant biomass is divided into four state variables (leaves, stems, roots and reserves). The latter is a pool to which biomass is allocated after allocations to leaves and stems that can later be remobilised to other plant parts (Höglind et al., 2001). Photosynthesis rate is the product of intercepted radiation and photosynthetic light-use efficiency, which takes into account carbon (C) losses through maintenance respiration. The latter depends on CO_2 concentration, through its effect on the photosynthesis rate at light saturation and CO_2 yield per photosynthetically active radiation, as well as air temperature, light intensity and the concentration of Rubisco (Rodriguez et al., 1999; Höglind et al., 2001). The model is based on the source-sink concept, where the source consists of photosynthesising tissue and C reserves, and the sink consists of newly developed above-ground plant parts and roots. Growth respiration is proportional to growth. The soil water is represented by one single layer and is affected by precipitation, runoff, evaporation and plant transpiration. In addition, root growth expands the volume of plant available water. See Höglind et al. (2001) and Höglind et al. (2016) for more details of the above mentioned processes. Simulations can be initialised in a growing sward either with small above ground plant parts early in the spring or after a cut, or with larger above ground plant parts later on in a growth cycle. The soil mineral nitrogen (N) pool that is avalible for plant uptake is, besides plant uptake, affected mineralisation of orgaincally bound N, N fertilisation and deposition, as well as by N losses through leaching and volatilisation processes. The part of the total soil mineral N pool that is avaliable is given by dividing it by a time constant. Given sufficient soil or shoot N available for remobilisation, the N remobilisation is determined by the difference between the actual plant N and the N that would be present if the shoot N followed the light extinction in the sward. Protein concentration is set to N concentration times 6.25. Cell wall content (i.e. fibre content) increases linearly with the plant development and can differ between leaves and stems, while the digestibility of cell wall decreases with the developmental stage. See Höglind et al. (2020) for more details about soil and plant N balance and processes. To simulate C and N dynamics in whole-crop barley in the present study, a spike state variable, equation for allocation of newly photosynthesised C to spikes were added together with cell wall content and digestibility of the spikes. Equations for translocation of C and N from stems and leaves to spikes and associated changes in the sward N canopy were also introduced. The model code can be downloaded from Zenodo (doi: 10.5281/zenodo.8275835). Details of these changes are provided in Sections 2.1.1 to 2.1.5.

2.1.1. Phenology

The parameter PHENGRAINFILL (unitless), which is the developmental stage (on a developmental stage scale from 0 to 1) that sets the start of the grain-filling period during which biomass is allocated to the spike pool, was introduced. PHENGRAINFILL also sets the start of transition of generative tillers, from which no allocation of C to spikes is possible (TILG2; m^{-2}), to tillers in which part of the C is allocated to the spikes (TILG3; m^{-2}).

Number of tillers, which transitions from the TILG2 to the TILG3 cohort (TILG2G3; m^{-2} d^{-1}) after the start of the grain-filling phase, is driven by a tiller transition rate parameter (RGRTG2G3; d^{-1}):

$$\mathrm{TILG2G3} = \mathrm{TILG2} * \mathrm{RGRTG2G3} \quad (1)$$

Relative death (senescence) rate of leaves due to phenological development (RDRPHEN; d^{-1}) is also initiated at the start of the grain-filling phase.

2.1.2. Carbon allocation and translocation to the spike pool

A state variable for spike C (CSPIKE; $g\ C\ m^{-2}$) was introduced to divide C between vegetative plant part (leaves and stems) and generative plant tissue (spikes). The increase in biomass in TILG3 tillers is driven by its sink strength (SINK2T; $g\ C\ tiller^{-1}\ d^{-1}$), which in turn is driven by the ratio between average spike C weight (CSPIKET; $g\ C\ tiller^{-1}$) and maximum possible spike C weight (CSPIKETM; $g\ C\ tiller^{-1}$):

$$SINK2T = \max(0\cdot,-1 - (CSPIKET/CSPIKETM))*SIMAX2T \quad (2)$$

where SIMAX2T ($g\ C\ tiller^{-1}\ d^{-1}$) is the sink strength of tillers in the TILG3 cohort at the start of grain filling. The change in sink strength during the grain-filling period is similar to the change in sink strength of tillers in the TILG2 cohort during the elongation phase, which is kept from the original BASGRA model (Höglind et al., 2016).

The direct allocation of C to spikes (ALLOSP; $g\ C\ m^{-2}\ d^{-1}$) is equal to the smallest of the total allocation of C to sinks (ALLOTOT; $g\ C\ m^{-2}\ d^{-1}$) and the potential direct allocation rate of C to spike mass (GSPSI; $g\ C\ m^{-2}\ d^{-1}$).

GSPSI is in turn given by:

$$GSPSI = \max(0\cdot, (SINK2T*TILG3*\ TRANRF\ *fSPIKE*\ NOHARV) / YG) \quad (3)$$

where TRANRF (unitless) is a transpiration realisation factor (unchanged from the original version of BASGRA), fSPIKE (unitless) is the maximum fraction of newly photosynthesised biomass or biomass mobilised from reserves that can go to the spike pool, NOHARV is an indicator of harvest given a value of 1 when there is no harvest and a value of 0 when the crop is harvested, and YG ($g\ C\ g\ C^{-1}$) is growth yield per unit of C expended.

The allocation of C to spikes (ALLOSP) is taken into account in the respiration of shoot growth (RESPGSH; $g\ C\ m^{-2}\ d^{-1}$) together with the allocation of C to leaves (ALLOLV) and stems (ALLOST):

$$RESPGSH = (ALLOLV + ALLOST + ALLOSP) * (1\text{-}YG) \quad (4)$$

The translocation of C from leaves to spikes (TRANSLLVSP) during the grain-filling period is set as a fraction of the death rate of the leaf mass up to a maximum translocation rate of C from leaves to spikes (TRANSLLVSPMAX; $g\ C\ m^{-2}\ d^{-1}$). However, the fraction of C in dying leaves that is translocated to spikes is reduced when the daily mean air temperature is above 23 °C or below 10 °C, based on Ritchie et al. (1985) and Pan et al. (2007). TRANSLLVSP is also subtracted from the translocation of C in dying leaves to the soil litter pool.

The translocation of C from stems to spikes is set as a fraction of C in stems per day determined by the relative translocation rate (RSTSPTRANSL; d^{-1}), as long as it is below the maximum stem to spike translocation (TRANSLSTSPMAX; $g\ C\ m^{-2}\ d^{-1}$). As done for leaf to spike C translocation, stem to spike translocation is reduced when the temperature is either above 23 °C or below 10 °C.

2.1.3. Harvest

The harvest equations in the original version of BASGRA were altered to include the tiller cohort with allocation of C and N to spikes (TILG3).

2.1.4. Nitrogen canopy dynamics, allocation and translocation

Plant N dynamics are included in the BASGRA_N version of the model (Höglind et al., 2020), where N content in the plant as a function of light extinction in crop canopy (which regulates plant growth) and N uptake from soil are set to stop at the start of grain filling. Three N state variables (N in stems (NSTEM; $g\ N\ m^{-2}$), N in leaves (NLEAF; $g\ N\ m^{-2}$) and N in spikes (NSPIKE; $g\ N\ m^{-2}$)) were added in this study to allow for N translocation from leaves and stems to spikes from the start of the grain-filling period. Protein content is calculated by multiplying the N content in each pool by 6.25. The translocation of N follows the same rules as the C translocation described above, but with separate parameters (Table 1) regulating the translocation rates (Table 2). The translocation of N from leaves to the soil N litter pool is set to stop at the start of grain filling.

Table 1
Parameters introduced in the BASGRA whole-crop model.

Parameter	Units	Explanation
CSPIKETM	$g\ C\ tiller^{-1}$	Maximum spike carbon (C) weight
DAYLG2G3	$d\ d^{-1}$	Day length above which tillers in TILG2 stage go into TILG3 stage
fDLVtransl	-	Fraction of C in dying leaves that is translocated to the spike pool
fDNLEAFtransl	-	Fraction of nitrogen (N) in dying leaves that is translocated to the spike pool
fSPIKE	-	Maximum fraction of newly photosynthesised biomass that can go to the spike pool
F_WALL_SPIKE_MAX	-	Maximum fraction of cell walls in spikes
F_WALL_SPIKE_MIN	-	Minimum fraction of cell walls in spikes
NCSHVEGMIN	-	Minimum N concentration in vegetative above-ground biomass
PHENGRAINFILL	-	Phenological stage above which C is allocated and translocated to the spike pool. The phenological developmental scale goes from 0 to 1
RDRPHENMX	d^{-1}	Maximum relative death rate of leaves due to phenology
RGRTG2G3	d^{-1}	Relative rate of tiller transitioning from the TILG2 to TILG3 cohort
RSTSPTRANSL	d^{-1}	Maximum relative translocation rate of stem C to spikes
RSTSPTRANSLN	d^{-1}	Maximum relative translocation rate of stem N to spikes
SIMAX2T	$g\ C\ tiller^{-1}\ d^{-1}$	Sink strength of tillers with allocation of C to spikes at the start of grain filling
TRANSLLVSPMAX	$g\ C\ m^{-2}\ d^{-1}$	Maximum translocation rate of C from leaves to spikes
TRANSLLVSPNMAX	$g\ N\ m^{-2}\ d^{-1}$	Maximum translocation rate of N from leaves to spikes
TRANSLSTSPMAX	$g\ C\ m^{-2}\ d^{-1}$	Maximum translocation rate of C from stems to spikes
TRANSLSTSPNMAX	$g\ N\ m^{-2}\ d^{-1}$	Maximum translocation of N from stems to spikes

2.1.5. Cell wall content and digestibility

Equations were added to describe the digestibility of the spike pool (F_DIGEST_SPIKE; unitless) and the fraction of spike DM that consists of cell wall (F_WALL_SPIKE; $g\ wall\ g^{-1}\ DM$). Similarly to the digestibility and cell wall content of other aboveground plant tissue, values of these variables change with phenological development stage. The digestibility of the spike pool increases as the fraction of chaff in the spike pool decreases (Slafer et al., 2002) and the fibre fraction in the grain decreases during the grain-filling period (Seog et al., 1993).

2.2. Model evaluation

2.2.1. Crop data

The BASGRA whole-crop model developed was calibrated and validated using data from field trials performed as part of the variety testing programme for cereal crops in Sweden (www.sortval.se). Validation data were excluded from the data that were used for the calibration of the model parameters. Data on DM weight, straw-leaf/spike ratio and nutritive value, including ash, crude protein, neutral detergent fibre (NDF) content and in vitro organic matter digestibility, were obtained for samples of two spring barley (*Hordeum vulgare* L.) cultivars (cv. Anneli and cv. Judit) taken at Zadoks growth stages 59, 75–77, 83–85 and 89 at Ås (63°15’N; 14°34’E), Lännäs (63°10’N; 17°38’E) and

Table 2
Variables introduced in the BASGRA whole-crop model.

Variable	Units	Explanation	Type
ALLOSP	$g\ C\ m^{-2}\ d^{-1}$	Allocation of carbon (C) to spikes	rate
ALLOSPN	$g\ N\ m^{-2}\ d^{-1}$	Allocation of nitrogen (N) to spikes	rate
CSPIKE	$g\ C\ m^{-2}$	Carbon in spikes	state
CSPIKET	$g\ C\ tiller^{-1}$	Average size of spike per tiller	intermediate
DMSPIKE	$g\ DM\ m^{-2}$	Spike dry matter	state
DNLEAF	$g\ N\ m^{-2}\ d^{-1}$	Decrease in N in leaves	rate
DNSPIKE	$g\ N\ m^{-2}\ d^{-1}$	Decrease in N in spikes	rate
DNSTEM	$g\ N\ m^{-2}\ d^{-1}$	Decrease in N in stem	rate
F_DIGEST_SPIKE	-	Digestibility of spikes	state
F_WALL_SPIKE	$g\ wall\ g\ DM^{-1}$	Fraction of spike dry matter that is cell wall	state
GNLEAF	$g\ N\ m^{-2}\ d^{-1}$	Increase in N in leaves	rate
GNSPIKE	$g\ N\ m^{-2}\ d^{-1}$	Increase in N in spikes	rate
GNSTEM	$g\ N\ m^{-2}\ d^{-1}$	Increase in N in stem	rate
GSPIKE	$g\ C\ m^{-2}\ d^{-1}$	Growth rate of spikes	rate
GSPSI	$g\ C\ m^{-2}\ d^{-1}$	Potential direct allocation rate of C to spikes	intermediate
GTILG2	$d^{-1}\ m^{-2}$	Increase in number of tillers	rate
HARVNLEAF	$g\ N\ m^{-2}\ d^{-1}$	Harvested leaf N	rate
HARVNSPIKE	$g\ N\ m^{-2}\ d^{-1}$	Harvested spike N	rate
HARVNSTEM	$g\ N\ m^{-2}\ d^{-1}$	Harvested stem N	rate
HARVSP	$g\ C\ m^{-2}\ d^{-1}$	Harvested spike C	rate
NSPIKE	$g\ N\ m^{-2}$	Nitrogen in spikes	state
NSTEM	$g\ N\ m^{-2}$	Nitrogen in stems	state
RDRPHEN	d^{-1}	Relative death rate of leaves due to phenology	intermediate
SINK2T	$g\ C\ tiller^{-1}\ d^{-1}$	Sink strength of tillers where C is allocated to spikes	intermediate
TILG2G3	$m^{-2}\ d^{-1}$	Transition rate of tillers from the TILG2 to TILG3 cohort	rate
TILG3	m^{-2}	Density of tillers with allocation of C to spikes	state
TRANSLLVSP	$g\ C\ m^{-2}\ d^{-1}$	Translocation rate of C from leaves to spikes	rate
TRANSLLVSPN	$g\ N\ m^{-2}\ d^{-1}$	Translocation of N from leaves to spikes	rate
TRANSLSTSP	$g\ C\ m^{-2}\ d^{-1}$	Translocation of C from stems to spikes	rate
TRANSLSTSPN	$g\ N\ m^{-2}\ d^{-1}$	Translocation of N from stems to spikes	rate

Röbäcksdalen (63°48’N; 20°12’E), Sweden (Fig. 1), in 2019 and 2020. In vitro organic matter digestibility was transformed to digestible organic matter in the DM (DOMD), according to Givens et al. (2009), by adding the ash content. The variety trial fields were sown in late May or early June, fertilized with between 80 kg N and 100 kg N around sowing, and when needed treated with a chemical herbicide a few weeks after emergence, following normal practices for northern Sweden and the weather conditions in 2019 and 2020. In addition, data on crop DM and nutritive value were taken from previous publications describing specifically designed whole-crop experiments on spring barley, as summarised in Table 3. For the location of the experimental sites see also Fig. 1. In total, those experiments included a wide range of soil and climate conditions, management practices and cultivars and encompassed a large part of the variation under which whole-crop barley is grown in northern Europe.

2.2.2. *Weather and soil data*

Daily weather data, including minimum and maximum temperatures, accumulated precipitation, global solar radiation, relative air humidity and average wind speed, measured at weather stations near the field experiments were downloaded from the open database of the Swedish Meteorological and Hydrological Institute (SMHI) (https://www.smhi.se/data/sa-anvander-du-tjansterna-for-oppna-data-1.145103) or from the LantMet network of weather stations administered by the Swedish University of Agricultural Sciences (SLU) (https://www.slu.se/fakulteter/nj/om-fakulteten/centrumbildningar-och-storre-forskningsplattformar/faltforsk/vader/lantmet/). Data on soil texture fractions were obtained from soil sampling at the trial sites and were used to calculate water-holding capacity characteristics (water content at wilting point, field capacity and saturation) used as input to the BASGRA model, applying methods in the SoilBuild tool (Saxton and Rawls, 2006) in DSSAT software v.4.7 (Hoogenboom et al., 2017). An overview of the climate and soil characteristics and management practices at the field trial locations is provided in Table 3.

2.2.3. *Calibration and validation settings*

Three model calibrations were carried out to determine model parameter values. Data from all locations were used in the first calibration, data from field trials in northern Sweden sampled in 2003, 2019 and 2020 were used in the second calibration, and data from the field trials at Alnarp, Götala, Kungsängen, Lanna and Rådde in central and southern Sweden were used in the third calibration (Table 4). The reason for this division of data was that there are physiological differences between varieties usually grown in northern and southern Sweden, notably differences in temperature requirement for phenological development (www.sortval.se) but also in traits that are related to other parameters whose effects on the evaluated outputs might be better represented if the calibration data is divided according to these geographic regions. In each calibration, the dataset was randomly divided into one subset for model calibration and one subset for model validation (Table 4). A proportion of the total dataset available for each calibration was not used for calibration, but instead used for model validation. These validation subsets consisted of 20%, 19% and 19% of the total data in the whole Sweden, northern Sweden and southern Sweden dataset respectively.

Bayesian calibration techniques as described by Van Oijen et al. (2005) and as previously applied on BASGRA (Höglind et al., 2020) were used. In Bayesian calibration, a prior distribution is updated based on observed data. In the present study, the prior distributions for parameters that were retained from the forage grass version of the BASGRA model were set as equal to the distributions used in a previous calibration against field trial data from northern Europe and Canada (Persson et al., 2019). The prior distributions (Appendix Table 1) of the plant parameters that were added in the BASGRA model version for whole-crop barley were set based on a combination of literature information (Slafer et al., 2002; Seog et al., 1993) (see also Section 2.1 for more information) and results from preliminary calibrations. Initial soil water characteristics were also treated as parameters and their prior distribution was set site-specifically according to soil texture characteristics. Sampling from the posterior distribution was made using the Metropolis algorithm and a chain length of 350000 simulation iterations. The likelihood function (Sivia, 2006) was applied. The model performance was validated using the maximum *a posteriori* (MAP) parameter values (Appendix Table 2). The simulations were initiated 14 days after sowing using very small initial values of initial leaf area (approximately 0.1 $m^2\ m^{-2}$) to represent a newly emerged crop.

2.3. *Yield and nutritive value under current and future climate conditions*

The variation in DM yield and nutritive value of whole-crop barley across climate zones and weather regions within Sweden was evaluated. For this evaluation, we applied the LARS WG tool (Semenov, 2008) v. 6.

Fig. 1. Experimental field locations.

First, Swedish Meteorological and Hydrological Institute (SMHI) daily data on minimum and maximum air temperature, precipitation, and solar radiation for Skara (58°23'N;13°27' E; 118 m asl), Umea (63°47'N; 20°17'E; 7 m asl) and Uppsala (59°53'N; 17°36'E; 17 m asl) and the period 1991–2022 were downloaded from the website of the Field Research Unit (Fältforsk) at SLU (https://www.slu.se/fakulteter/nj/om-fakulteten/centrumbildningar-och-storre-forskningsplattformar/faltforsk/vader/lantmet/). Second, site information and data files were created according to the manual included in LARS-WG v. 6. Third, a site analysis to analyse dry and wet spells, and cold and hot spells for the three sites. Finally, for each of the three locations, 100 years of synthetic daily data on minimum and maximum air temperature, precipitation, and solar radiation were generated for the baseline period, and for the time period 2021–2040 and the Global climate model Hadley Centre Global Environment Model version 2 (HadGEM2-es) and the representative concentration pathway (RCP 4.5). The latter represents a moderate greenhouse gas emission scenario, which includes an average global warming of 1.5 °C (IPCC, 2013) and approximately 2 °C in Northern Europe (Hansen-Bauer et al., 2015) compared to the temperatures during the late 20th century and early 21st century. The climate changes for northern Europe associated with RCP 4.5 also include increases in annual precipitation until 2050 (Hansen-Bauer et al., 2015). The sets of generated weather data can be considered to represent the variation in the weather under conditions ranging from recent historical to near-future with no stringent mitigation of greenhouse gas emissions. Using 100 years of synthetic weather data for both time periods also meant that we compared the same number of repetitions within each combination of time and location.

Dry matter yield and nutritive value attributes were then simulated using the MAP parameter values from the whole Sweden calibration and the generated weather data as input. For each of the three locations (Skara, Umeå and Uppsala), 100 years of simulations were performed using weather data representing 1990–2020 climate conditions and the 2021–2040 HadGEM2-es and RCP4.5 climate. For the latter conditions, the CO_2 concentration in BASGRA was changed from 350 to 435 ppm in accordance with RCP 4.5 (IPCC, 2013). Initialisation date was set to the first day after which mean daily temperature exceeded 5.0 °C for five consecutive days using the same initial leaf area as in the calibrations.

Table 3
Climate, soil characteristics and management practices at the experimental locations.

Name	Location	Mean annual temperature (°C)	Mean annual accumulated precipitation (mm)	Soil type	Experimental year	Cultivar	N fertiliser dose (kg ha^{-1})	Reference
Ås	63°15'N; 14°34'E; 374 m asl	3.7 °C	503.3	Loam	2019-20	Anneli, Judit	80	-
Lännäs	63°10'N; 17°38'E; 20 m asl	3.8 °C	594.4	Silt loam-loam	2019-20	Anneli, Judit	100	-
Röbäcksdalen	63°48'N; 20°12'E; 20 m asl	4.1 °C	671.8	Silt loam	2003, 2019-20	Anneli, Judit, Olsok	72 kg N 2003; 100 kg N 2019 and 2020	(Wallsten et al., 2009; Wallsten et al., 2010) 2003 experiment
Alnarp	55°39''N; 13°04' E	8.8 °C	612	Sandy loam	2003	Pasadena	100	(Wallsten et al., 2009; Wallsten et al., 2010)
Götala	58°23' N; 13°29' E; 120 m asl	7.1 °C	665.5	Sandy loam	2003	Kinnan	100	(Rustas et al., 2011)
Kungsängen	59°50' N; 17°40' E; 2 m asl	6.7 °C	540.6	Clay loam	2003	Filippa	70	(Rustas et al., 2011)
Lanna	58°21' N; 13°07' E; 73 m asl	7.3 °C	583.7	Clay	2003	Henny	120	(Nadeau, 2007)
Rådde	57°60′N; 13°25′E	6.3 °C	968.3	Moraine sand	2006-07	Baronesse, Kinnan, Orthega, Otira, Sebastian	90	(Nadeau and Jansson, 2010)

Table 4
Calibration and validation datasets.

Location	Year	Cultivar	Developmental stage at cutting[a]	All Sweden data	Northern Sweden data	Southern Sweden data
Alnarp	2003	Pasadena	71, 83	Calibration	-	Validation
Götala	2003	Kinnan	73, 85	Calibration	-	Calibration
Kungsängen	2003	Filippa	65, 75	Validation	-	Calibration
Lanna	2003	Henny	73, 83	Calibration	-	Calibration
Röbäcksdalen	2003	Olsok	59, 73, 83	Calibration	Calibration	-
Rådde	2006	Baronesse	73	Validation	-	Calibration
Rådde	2006	Kinnan	75	Calibration	-	Calibration
Rådde	2006	Orthega	76	Calibration	-	Calibration
Rådde	2006	Otira	75	Calibration	-	Validation
Rådde	2006	Sebastian	75	Calibration	-	Calibration
Rådde	2007	Baronesse	72	Calibration	-	Calibration
Rådde	2007	Kinnan	74	Calibration	-	Validation
Rådde	2007	Orthega	75	Calibration	-	Calibration
Rådde	2007	Otira	76	Calibration	-	Calibration
Rådde	2007	Sebastian	76	Calibration	-	Calibration
Ås	2019	Anneli	59, 75-77, 83-85, 89	Calibration	Calibration	-
Ås	2019	Judit	59, 75-77, 83-85, 89	Calibration	Validation	-
Lännäs	2019	Anneli	59, 75-77, 83-85, 89	Calibration	Calibration	-
Lännäs	2019	Judit	59, 75-77, 83-85, 89	Calibration	Calibration	-
Röbäcksdalen	2019	Anneli	59, 75-77, 83-85, 89	Validation	Calibration	-
Röbäcksdalen	2019	Judit	59, 75-77, 83-85, 89	Calibration	Calibration	-
Ås	2020	Anneli	59, 75-77, 83-85, 89	Calibration	Calibration	-
Ås	2020	Judit	59, 75-77, 83-85, 89	Calibration	Calibration	-
Lännäs	2020	Anneli	59, 75-77, 83-85, 89	Validation	Calibration	-
Lännäs	2020	Judit	59, 75-77, 83-85, 89	Calibration	Validation	-
Röbäcksdalen	2020	Anneli	59, 75-77, 83-85, 89	Calibration	Calibration	-
Röbäcksdalen	2020	Judit	59, 75-77, 83-85, 89	Calibration	Calibration	-

[a] According to the scale developed by Zadoks et al. (1974).

Four cutting times, which represented the crop developmental stages at cutting in the experiments from 2019 and 2020 (see Section 2.2.1), were simulated. A fertiliser dose of 100 kg N ha^{-1} was applied at the start of the simulations in spring in both climate scenarios, at all locations and for all four cutting regimes.

2.4. Statistical analysis

The ability of the model to predict nutritive components (crude protein, NDF, DM digestibility) was evaluated using root mean squared error (RMSE):

$$RMSE = \sqrt{\frac{\sum_{i=1}^{n} (P_i - O_i)^2}{n}} \tag{5}$$

where n is the number of observations and P_i and O_i are the predicted and observed values for each data pair. The closer the RMSE is to 0, the better the prediction. RMSE was normalised by dividing it by the mean value of the observations.

Relative mean bias error (rMBE) was calculated to provide a measure of the relative magnitude of misprediction (over- or under-prediction):

Table 5

Statistics for the whole Sweden calibration. Observed and simulated means, root mean squared error (RMSE), normalised RMSE, relative mean bias error (rMBE) and Willmott's index of agreement (d-index) for biomass crude protein (CP) concentration, neutral detergent fibre (NDF) concentration and digestible organic matter in the dry matter (DOMD).

	Number of observations	Mean of observations	Mean of simulations	RMSE	Normalised RMSE (%)	rMBE (%)	d-index
Calibration							
Biomass (g DM m^{-2})	53	655.2	618.9	182.2	27.8	-5.54	0.609
CP concentration (g g^{-1} DM)	58	0.100	0.0986	0.0204	20.4	-1.64	0.597
NDF concentration (g g^{-1} DM)	58	0.494	0.512	0.0524	10.6	3.69	0.794
DOMD (g g^{-1} DM)	58	0.722	0.799	0.0886	12.3	10.7	0.416
Validation							
Biomass (g DM m^{-2})	10	600.5	590.9	124.8	20.8	-1.61	0.733
CP concentration (g g^{-1} DM)	13	0.0988	0.0921	0.0262	26.5	-6.82	0.893
NDF concentration (g g^{-1} DM)	13	0.486	0.496	0.0322	6.63	1.92	0.942
DOMD (g g^{-1} DM)	13	0.722	0.802	0.0927	12.8	11.1	0.430

Table 6

Statistics for the northern Sweden calibration. Observed and simulated means, root mean squared error (RMSE), normalised RMSE, relative mean bias error (rMBE) and Willmott's index of agreement (d-index) for biomass crude protein (CP) concentration, neutral detergent fibre (NDF) concentration and digestible organic matter in the dry matter (DOMD).

	Number of observations	Mean of observations	Mean of simulations	RMSE	Normalised RMSE (%)	rMBE (%)	d-index
Calibration							
Biomass (g DM m^{-2})	40	658.5	637	169.9	25.8	-3.23	0.614
CP concentration (g g^{-1} DM)	43	0.107	0.102	0.0188	17.6	-5.10	0.678
NDF concentration (g g^{-1} DM)	43	0.483	0.528	0.0668	13.8	9.47	0.768
DOMD (g g^{-1} DM)	43	0.710	0.798	0.0964	13.6	12.5	0.418
Validation							
Biomass (g DM m^{-2})	8	547.1	665.2	185.8	27.9	21.6	0.776
Crude protein (g g^{-1} DM)	8	0.0998	0.102	0.0239	24.0	1.87	0.856
Neutral detergent fibre (g g^{-1} DM)	8	0.491	0.526	0.0523	10.7	7.17	0.821
DOMD (g g^{-1} DM)	8	0.729	0.796	0.0771	10.6	9.13	0.465

Table 7

Statistics for the southern Sweden calibration. Observed and simulated means, root mean squared error (RMSE), normalised RMSE, relative mean bias error (rMBE) and Willmott's index of agreement (d-index) for biomass crude protein (CP) concentration, neutral detergent fibre (NDF) concentration and digestible organic matter in the dry matter (DOMD).

	Number of observations	Mean of observations	Mean of simulations	RMSE	Normalised RMSE (%)	rMBE (%)	d-index
Calibration							
Biomass (g DM m^{-2})	13	682.8	651.8	115.8	17.0	-4.54	0.834
CP concentration (g g^{-1} DM)	16	0.0809	0.0753	0.0125	15.5	-6.87	0.531
NDF concentration (g g^{-1} DM)	16	0.517	0.527	0.0392	7.58	1.86	0.184
DOMD (g g^{-1} DM)	16	0.747	0.906	0.166	22.2	21.4	0.319
Validation							
Biomass (g DM m^{-2})	2	570.0	579.6	19.90	3.5	1.68	0.943
CP concentration (g g^{-1} DM)	4	0.101	0.0781	0.0322	32.0	-22.5	0.722
NDF concentration (g g^{-1} DM)	4	0.501	0.529	0.0586	11.7	5.69	0.283
DOMD (g g^{-1} DM)	4	0.744	0.906	0.163	21.9	21.8	0.0960

$$rMBE = \frac{\sum_{i=1}^{n}(P_i - O_i)}{\sum_{i=1}^{n} O_i} \tag{6}$$

Willmott's index of agreement as a complementary statistical metric was also calculated:

$$d = 1 - \left[\frac{\sum_{i=1}^{n}(P_i - O_i)^2}{\sum_{i=1}^{n}(|P'_i| + |O'_i|)^2}\right] \tag{7}$$

where P_i’ is P_i’M and O_i’ is O_i-M, M is the mean of the observed values and d can take a value from 0, which indicates no agreement at all between observed and simulated values, and 1, which indicates complete agreement (Willmott, 1982).

For the 100-year simulations, the difference in mean DM yield, crude protein and NDF content and DOMD between locations, climate projections and cutting times was assessed by one-way analysis of variance (ANOVA) and Fischer's least significant difference (LSD), using PROC GLM in SAS v 9.4 (SAS Institute Inc, 2020). Differences between locations were analysed within climate projections and cutting times, differences between climate projections within locations and cutting times, and differences between cutting times within locations and climate projections.

3. Results

3.1. Model calibration and validation

The prediction accuracy for NDF concentration in whole-crop barley (normalised RMSE 7.58–13.8%) and DOMD (12.3–21.4%) was generally higher than the prediction accuracy for crude protein concentration (17.6–23.2%) and biomass (17.0–27.8%) for the parameter sets based on the three calibrations. Willmott's index of agreement indicated more fluctuating prediction accuracy between crop characteristics and calibrations. The trends in prediction accuracy found in validation of these calibrations, as evaluated by the same metrics, were similar (Tables 5–7). Biomass and crude protein tended to be underpredicted in both calibrations and validations, whereas NDF and DOMD were overpredicted in both calibrations and validations, as evaluated by rMBE.

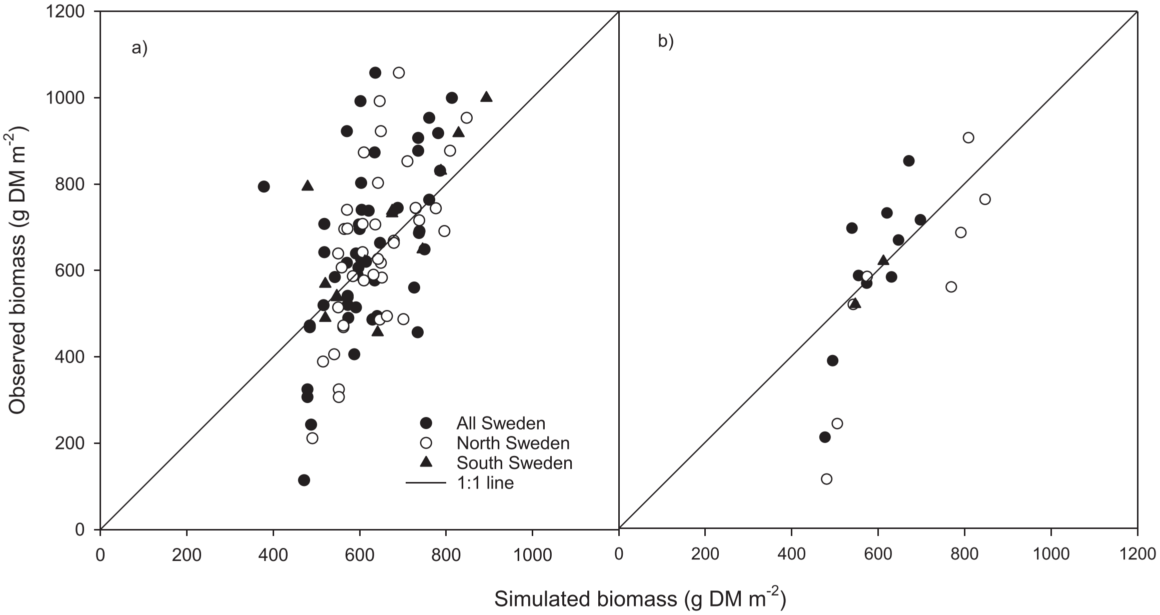

Fig. 2. Observed biomass plotted against simulated biomass for the three a) model calibrations and b) model validations. Statistics on calibrations and validations are presented in Tables 5–7.

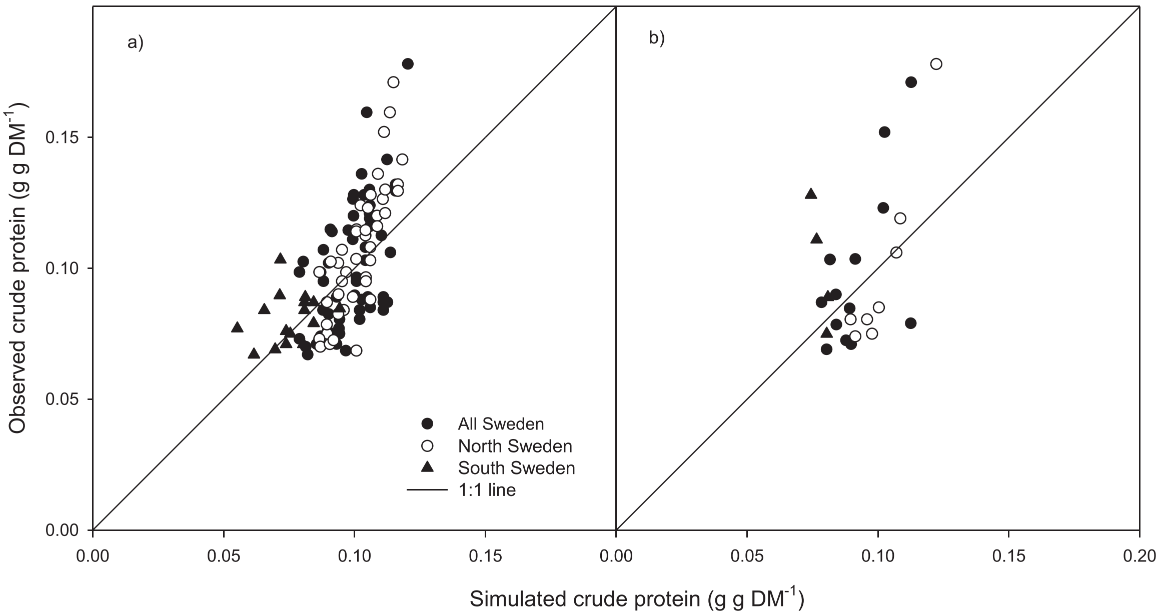

Fig. 3. Observed crude protein plotted against simulated crude protein for the three a) model calibrations and b) model validations. Statistics on calibrations and validations are presented in Tables 5–7.

Apart from these differences, it was not possible to discern any trends in prediction accuracy between the calibrations and validations for any of the crop characteristics evaluated (see Tables 5–7 and Figs. 2–5 for more details). The prediction accuracy of DOMD was considerably lower for the southern Sweden parameter set than for the other parameters sets, as evaluated by normalised RMSE. For the other variables, there were no clear trends in prediction accuracy between the parameter sets.

3.2. Yield and nutritive value under current and future climate conditions

Dry matter yield was significantly lower under the 2021–2040 climate (mean 658.8 g DM m^{-2} across cutting times and locations) than under the 1990–2020 climate (mean 678.9 g DM m^{-2} across cutting times and locations) at all four cutting stages and at all three locations (Table 8). The NDF concentration tended to be slightly higher and DOMD slightly lower under the 2021–2040 climate than under the 1990–2020 climate while the effect of climate on crude protein concentration was more variable across locations (Figs. 6–8). Dry matter yield increased, while crude protein concentration, NDF concentration and DOMD decreased with increasing development stage under both climate scenarios and at all locations, i. e. there was a negative relation between dry matter and the three nutritive value components. For both climate scenarios and at all development stages at cutting, dry matter yield was significantly higher at Skara than at the other two locations and mostly significantly higher at Uppsala than at Umeå, across climate scenarios and cutting stages. Crude protein concentration was significantly higher at Uppsala than at Skara and Umeå but mostly not significantly different between the other two locations, whereas NDF

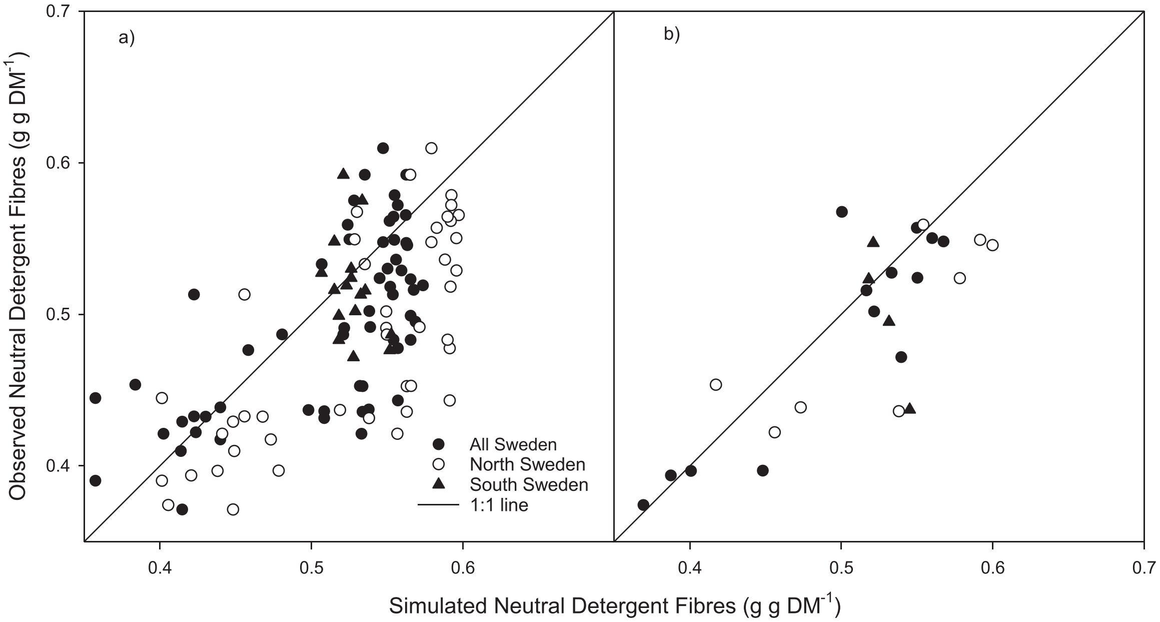

Fig. 4. Observed neutral detergent fibre (NDF) plotted against simulated NDF for the three a) model calibrations and b) model validations. Statistics on calibrations and validations are presented in Tables 5–7.

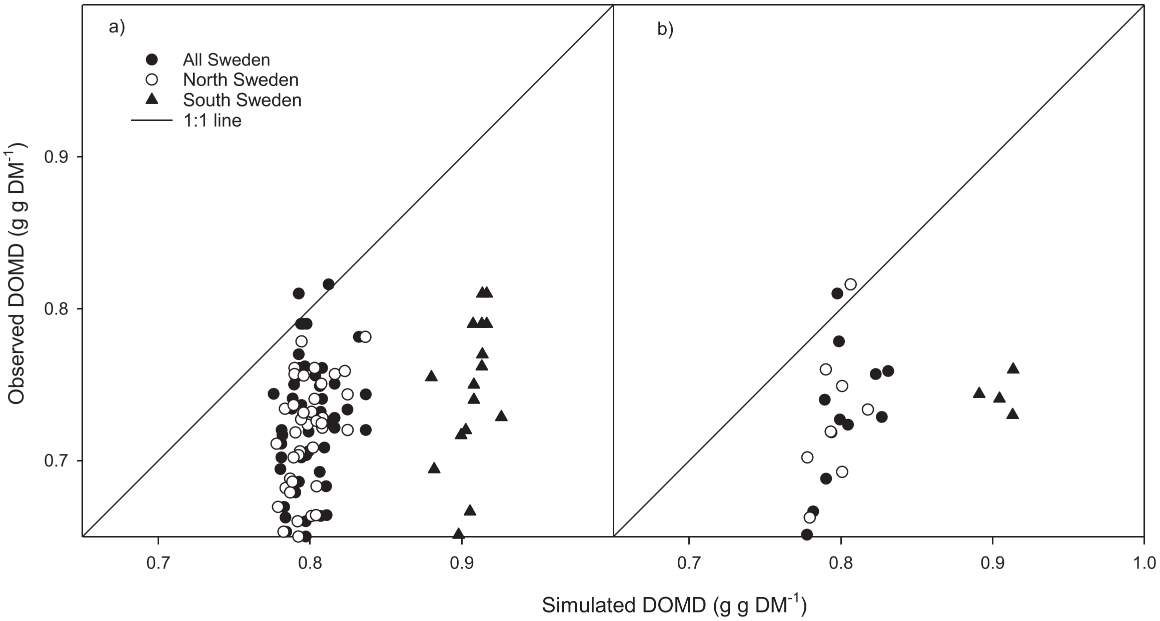

Fig. 5. Observed digestible organic matter in the dry matter (DOMD)plotted against simulated DOMD for the three a) model calibrations and b) model validations. Statistics on calibrations and validations are presented in Tables 5–7.

concentration was significantly higher at Skara and Uppsala than at Umeå at most development stages under both climate scenarios. Digestible organic matter in the DM tended to be highest at Umeå and second highest at Skara for all cutting stages and both climate scenarios. Fig. 9.

All cuttings occurred at earlier dates under the 2021–2040 climate scenario than under the 1990–2020 scenario. The differences in cutting dates between climate scenarios were generally higher at Umeå (on average between 9 and 16 days) than at Skara (on average between 7 and 9 days) and Uppsala (on average between 8 and 9 days) and also tended to be higher at later developmental stages than at earlier stages. Moreover, the cutting date varied less under the 2021–2040 climate scenario than under the 1990–2020 climate scenarios, especially at Umeå (Fig. 5).

4. Discussion

4.1. Model performance

In this study the BASGRA model, which was originally developed for forage grass, was adjusted to simulate yield and nutritive value attributes of whole-crop barley under a range of environmental conditions and genetic diversity. There are several possible reasons for the fact that the prediction accuracy was generally higher for NDF, and partly also for crude protein and DM yield, than for DOMD. First, the high prediction accuracy of NDF could be related to lower genetic variability in the plant

Table 8
Effect of climate projections on dry matter yield (g DM m^{-2}) of whole-crop barley cut at different developmental stages.

	Skara[a]	Umeå	Uppsala
Heading stage			
1990-2020	692.9 b	643.1 b	659.4 b
2021-2040	680.1 a	624.4 a	642.3 a
Milk stage			
1990-2020	701.4 b	650.6 b	665.0 b
2021-2040	688.9 a	631.5 a	647.4 a
Dough stage			
1990-2020	716.6 b	663.1 b	674.0 b
2021-2040	696.1 a	641.8 a	655.2 a
Hard dough stage			
1990-2020	726.6 b	674.1 b	679.8 b
2021-2040	704.4 a	647.3 a	659.7 a

[a] Different letters within cutting stage and location indicate statistically significant differences ($p < 0.05$).

functions that regulate this nutritive value attribute across cultivars than in those regulating biomass, crude protein content and digestibility. The overall higher prediction accuracy of NDF than of crude protein is in line with findings in a previous evaluation of the BASGRA CATIMO and STICS forage grass models for timothy grass (Persson et al., 2019; Bonesmo and Belanger, 2002a; Bonesmo and Belanger, 2002b; Jégo et al., 2013), indicating that prediction accuracy for NDF is rather stable across grass ley and cereal crops, while the low prediction accuracy of digestibility differs from findings for timothy grass in the evaluation of the same forage grass models (Persson et al., 2019). There was greater variation of biomass within many of the datasets used than within the measured nutritive value attributes (data not shown), suggesting that the former observations were associated with greater uncertainty, which may explain some of the biomass prediction error. Possible measurement errors could also have contributed to the high variability in observed biomass since, especially in uneven stands, there is arguably a higher risk of obtaining non-representative biomass weight samples than nutritive value attribute samples. A greater variation in observed biomass than in observed nutritive value has also been found in previous studies of forage grass (Bélanger et al., 2008; Nissinen et al., 2010).

4.2. Regional differences

That the prediction accuracy in the northern Sweden calibration was not better than that in the calibration for the whole country could be

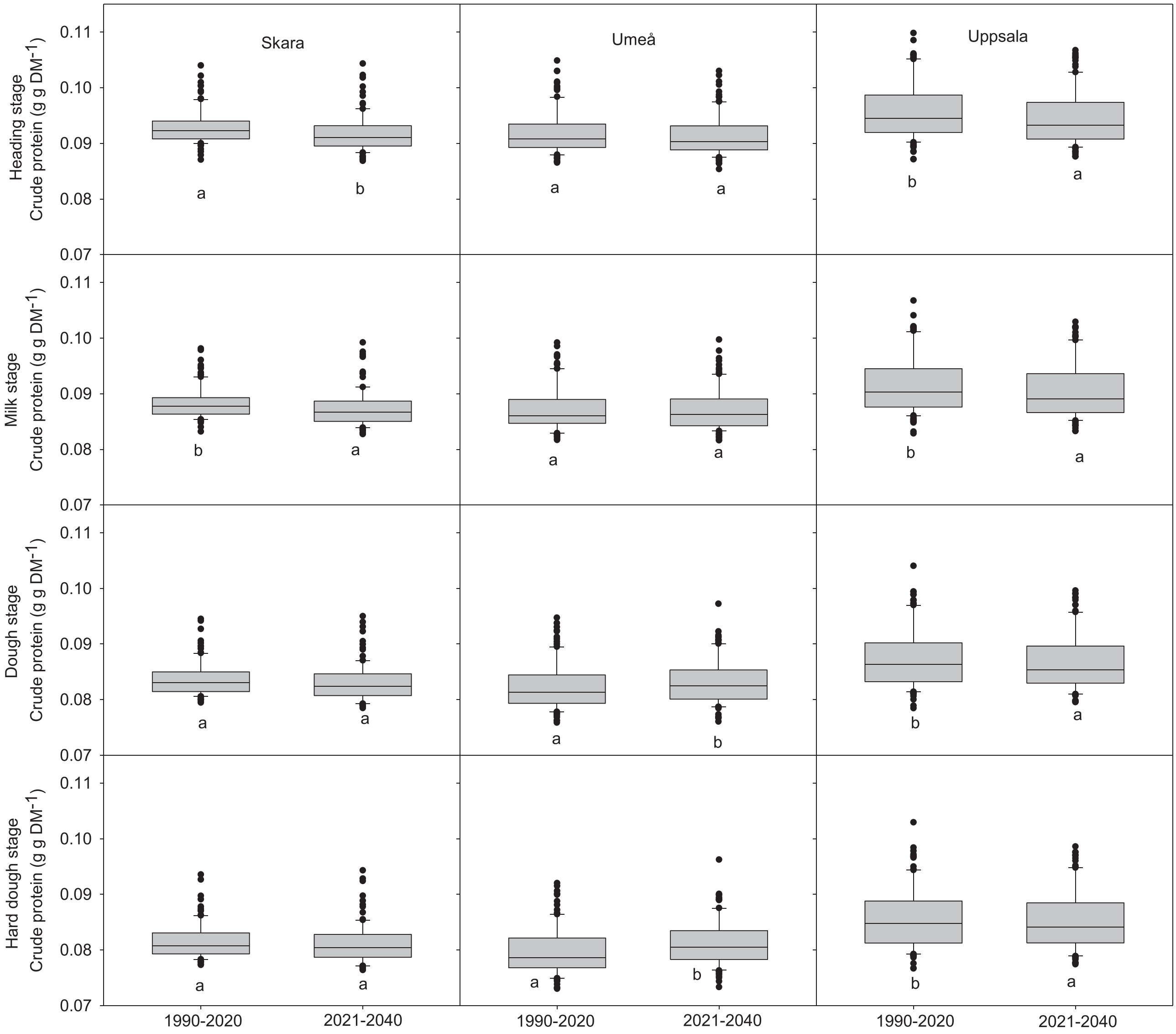

Fig. 6. Crude protein concentration in the 100-year simulations using historical (1990–2020) and near-future (2021–2040) data. Whiskers represent 5th/95th percentile and outliers are represented by dots.

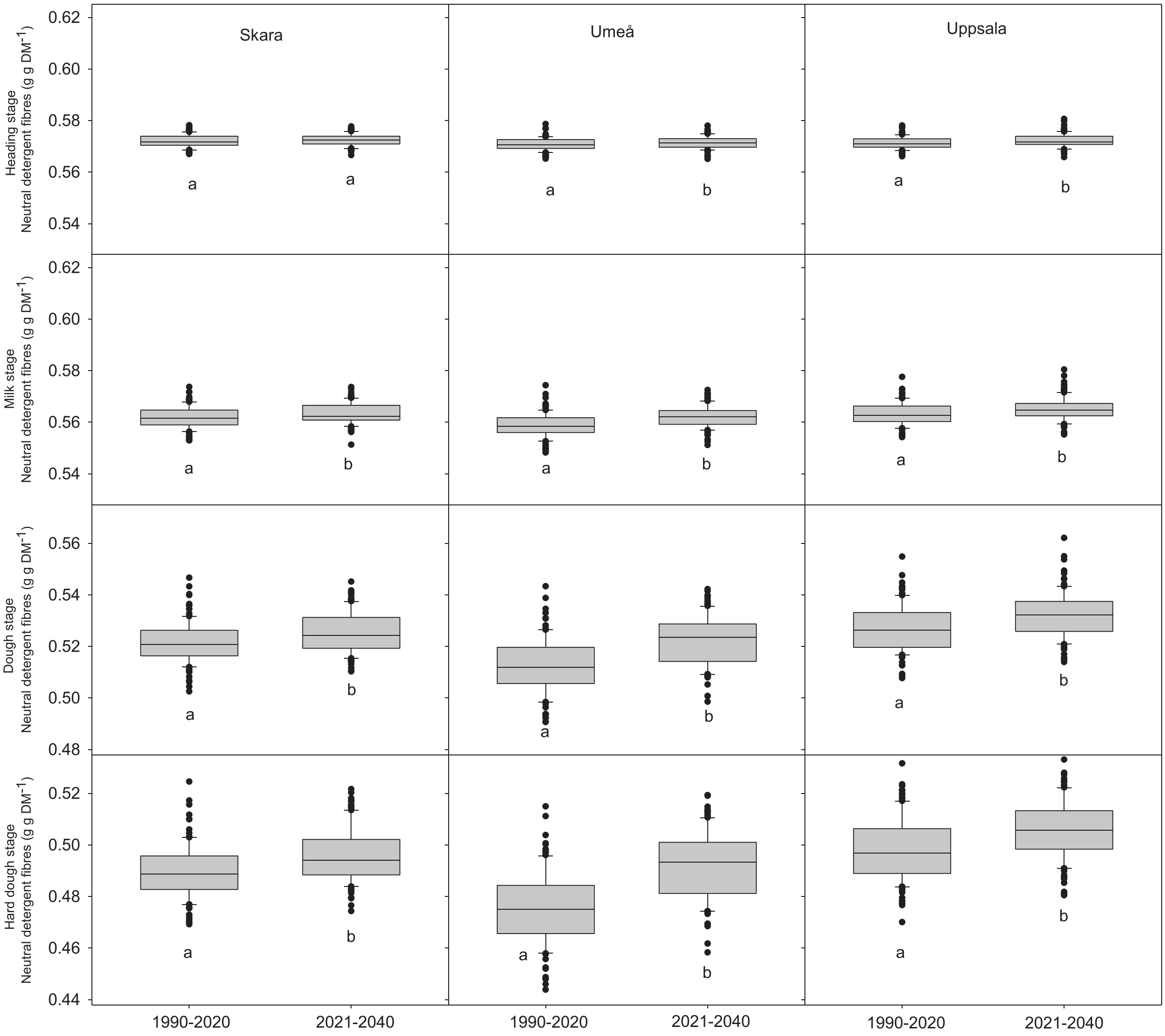

Fig. 7. Neutral detergent fibre concentration in the 100-year simulations using historical (1990–2020) and near-future (2021–2040) data. Whiskers represent 5th/95th percentile and outliers are represented by dots.

because to physiological differences within the former dataset have a larger impact on the model performance than physiological differences between cultivars at the northern and southern locations or environmental differences between geographic regions that are not fully mechanistically accounted for in the BASGRA model. The fact that there was one two-row barley cultivar (Anneli) and two six-row barley cultivars (Judit and Olsok) in the northern Sweden dataset with different physiological traits supports this argumentation. More data than what was available for this study would be needed to test if the effect of cultivar-specific calibration could improve prediction accuracy. The southern Sweden calibration dataset consisted of a wide range of cultivars with different properties, which could likewise explain why this calibration did not improve the prediction accuracy compared with the calibration for the whole country. The lack of effect of geographical region used in calibration on model performance differs from findings in previous model calibrations for wheat (Hao et al., 2021) and forage grass (Persson et al., 2014), in which the yield predictions increased after site-specific factors were taken into account. These differences in regional effect between crops could be due to a higher geographic variability in stressors and other factors affecting winter wheat and perennial forage grasses but not whole crop spring barley, notably winter stress, which is not described with a very high level of details in most cereal crop (Hochman et al., 2013; Bergjord Olsen et al., 2018) and forage grass models (Kipling et al., 2016). Overall, this indicates that regional specific whole crop model calibrations taking into account variations in climate, soil and other environmental factors should be combined with other measures. These include division of datasets into specific cultivars, climate and soil conditions, requiring larger sets of cultivar and site-specific data than were used in this study. Moreover, both protein and fibre concentration, and digestibility of stems and leaves (Bonesmo and Belanger, 2002b; Nissinen et al., 2010) have been shown to vary considerably between environmental conditions and developmental stages in other grass species than barley. Hence, nutritive value specifically for stems and leaves, as well as for spikes could be useful in understanding the effect of C and N allocation and translocation on the change in nutritive value during plant development, especially the reason for overprediction of DOMD and underprediction of crude protein content.

4.3. *Practical applications*

Apart from DOMD, the prediction accuracy was sufficiently high for the modified model to be useful in evaluating the performance and composition of whole-crop barley under different production conditions in Sweden or other countries with similar climate, soil and crop management practices. The higher prediction accuracy for NDF than for

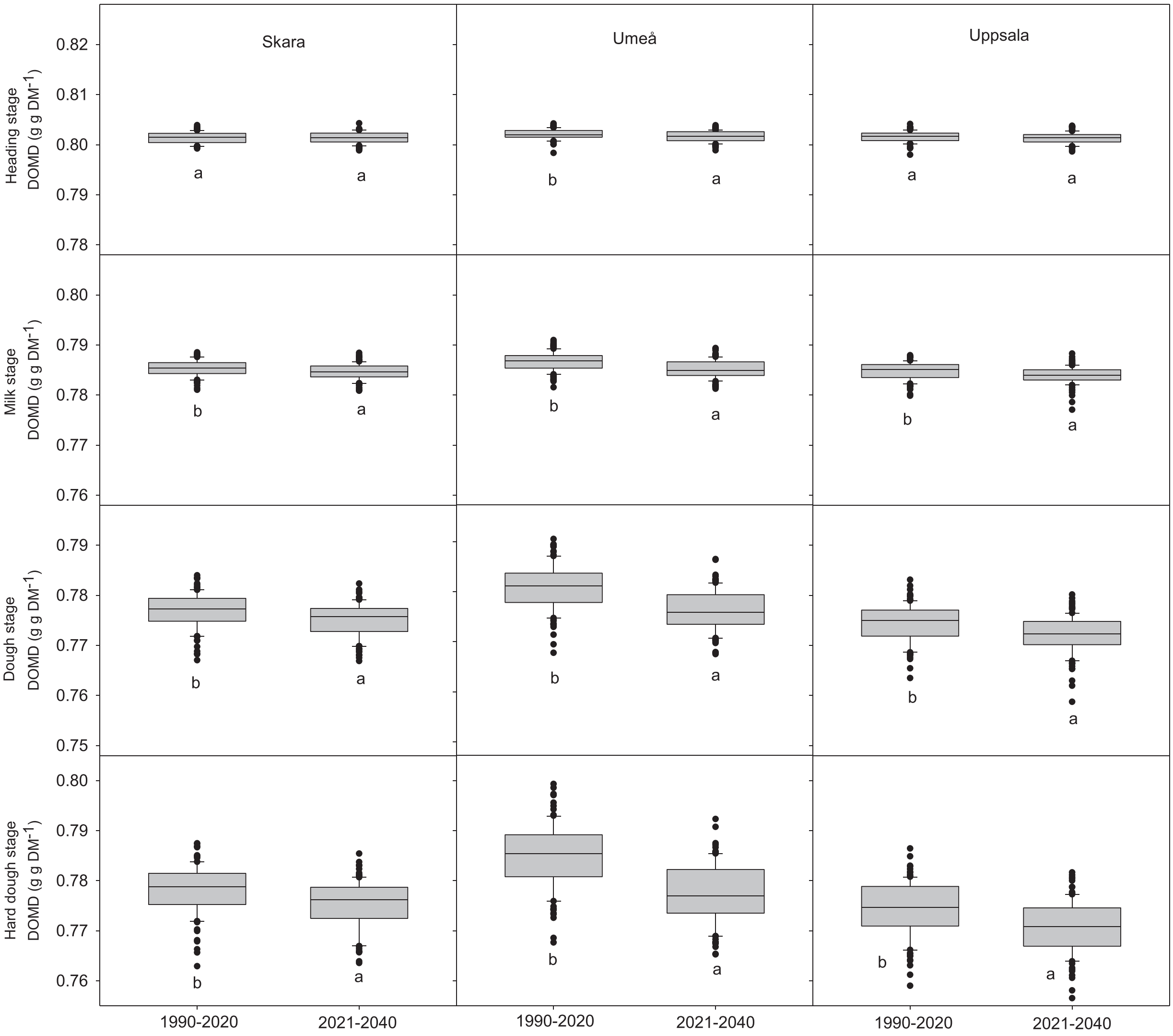

Fig. 8. Digestible organic matter in the dry matter (DOMD) in the 100-year simulations using historical (1990–2020) and near-future (2021–2040) data. Whiskers represent 5th/95th percentile and outliers are represented by dots.

crude protein and biomass could be important in applications of the model in e. g. forecasting systems for forage production. In ruminant feeding regimes, the fibre component, which gives structure to the diet (Banakar et al., 2018), is usually mainly supplied by forage, e. g. whole-crop barley. Still, at advanced developmental stages, a reduction of the NDF concentration promotes higher intake, which to some extent can compensate for a relatively low energy content (Rustas et al., 2010). The protein requirement of cattle and other ruminants is largely covered by feed components such as grass-legume silage (Castro-Montoya and Dickhoefer, 2020; Chowdhury et al., 2023) and concentrate (Wilkinson, 2011; Erickson and Kalscheur, 2020), which is also true in feeding regimes that include whole crop components, especially when the whole crop is cut at a late developmental stage (Hetta et al., 2012; Wallsten et al., 2009).

4.4. Climate impact on whole crop production

The rather small differences in NDF, DOMD, crude protein and biomass between locations and climate conditions in the 100-year simulations suggest that production of whole-crop barley is rather stable under the conditions studied and under regional climate conditions representing the near future. However, the small negative impact of climate change on dry matter yield differs from simulated positive effects of climate change on forage grass yield, largely as an effect of longer growing seasons in the same geographic region (Höglind et al., 2013). The simulated earlier cutting dates and lower cutting date variability under the 2021–2040 climate than under the 1990–2020 also indicate that the changing climate could allow for more cropping flexibility. This flexibility gives a longer time for field preparation and sowing in the spring, which can be a particular bottleneck in high-latitude regions with relatively high precipitation (Kolberg et al., 2019). It also gives a longer time for winter crop sowing in autumn, provided that projected future increases in precipitation and higher frequency of extreme precipitation events (Lehtonen et al., 2014) do not impair the conditions for seedbed preparation and sowing. The slightly lower yield, which possibly could be due to a shorter period for carbon assimilation which in turn can be a result of faster phenological development (Tao et al., 2008; Fatima et al., 2020) may also to some extent limit future whole crop production.

4.5. Further research priorities

This study adds to previous findings on the sensitivity of cereals and other agricultural crops to weather and climate variability, which have focused mainly on yield quantity (Tripathi et al., 2016; Wang et al., 2018) and to some extent on N and protein (Asseng et al., 2019), but

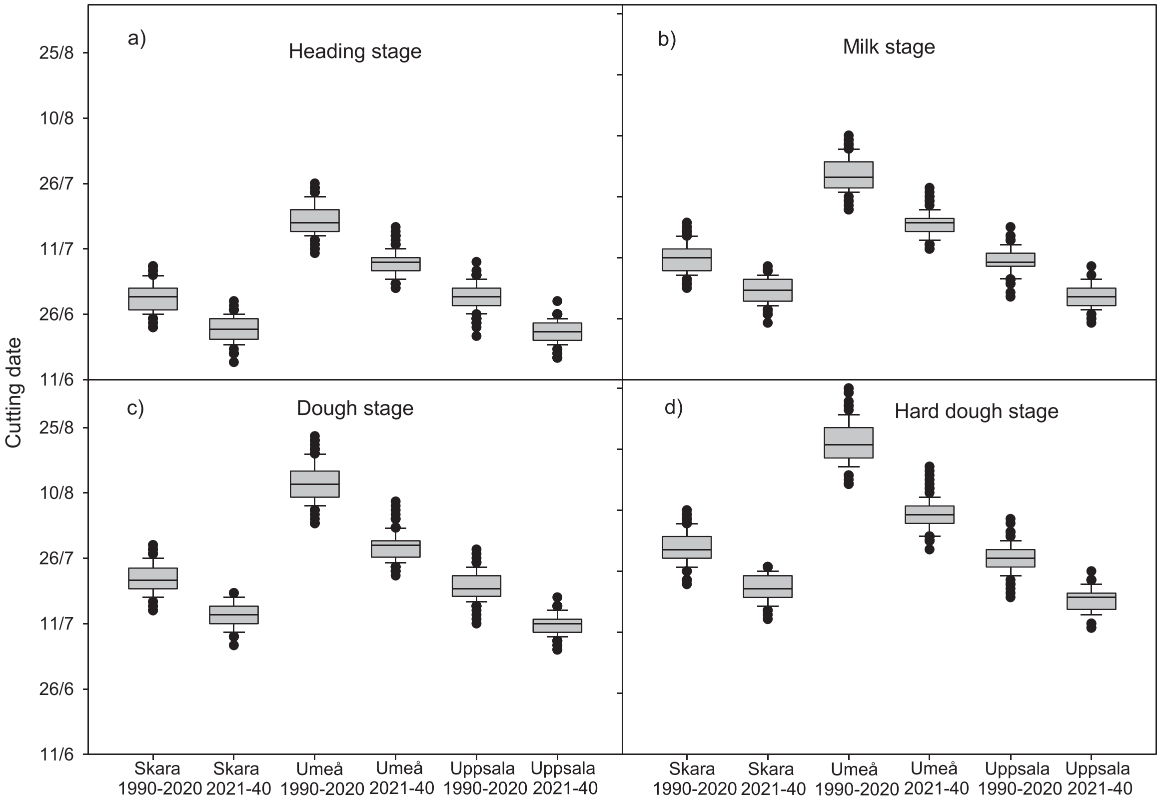

Fig. 9. a) Heading stage (Zadoks 59), b) milk stage (Zadoks 75–77, c) dough stage (Zadoks 83–85) and d) hard dough stage (Zadoks 89) cutting dates in the 100-year simulations using historical (1990–2020) and near-future (2021–2040) data. Whiskers represent 5th/95th percentile and outliers are represented by dots.

have largely excluded other quality aspects. However, there are also reasons to treat the results from our study with some caution. Climate projections differing from that considered here might have generated different results given the large impact of climate projections and global climate models found on other crops such as grain cereals (Challinor et al., 2009; Asseng et al., 2013) and forage grass (Graux et al., 2013; Höglind et al., 2013). The deviation between simulated and observed variables, in particular the overprediction of digestibility, suggests a need for further model development before future evaluations of climate impact, e.g. including a wider range of climate change projection, on whole-crop barley production. This could also include sensitivity tests to dry and wet spells, as adjusted by LARS-WG or another weather generator, to further emphasize risks and preparation for worse case scenarios for seed bed preparation, sowing and harvest. Such efforts could also take into account a wider geographic selection of locations, soil properties and management practices, notably N fertilisation, which are representative of Sweden and other regions where whole crop barley is commonly grown or has a potential to become an important animal feed component. Such an approach could improve the prediction accuracy and improve understanding of changes in whole-crop production due to climate change and other environmental variation in an applied perspective. Further research tasks to improve model prediction accuracy could include calibrations based on cultivar differences (e.g. between two-row and six-row barley cultivars) and detailed studies about N and C translocation between vegetative biomass and spikes and its link to changes in fibre concentration and digestibility during crop development. Such studies could be accompanied by future scenario analyses and piecemeal implementation of the model in decision support systems for famers and agricultural advisors.

5. Conclusions

The BASGRA model for forage grass was adapted to simulate whole-crop barley, notably by adding a spike pool, equations for C and N allocation to the spike pool and equations for C and N translocation from vegetative plant parts to spikes. Model calibrations and validations using field trial data from across Sweden, and across crop developmental stages from late anthesis to hard dough, generally showed better prediction accuracy of nutritive value attributes, especially NDF, than of DM yield. Except in the case of DOMD, prediction accuracy was sufficiently high to allow the model to be used for evaluating the performance of whole-crop barley under different production conditions in Sweden. Region-specific calibrations for southern and northern Sweden did not change the pattern of prediction accuracy. An evaluation of climate change effects showed lower DM yield, earlier harvest and slightly higher NDF concentration on average for 100 years of generated weather data representing near-future climate conditions (2021–40) than data representing historical climate conditions (1990–2020) at three locations in Sweden (Skara, Umeå and Uppsala), using the model version calibrated against the dataset for the whole country. Further model development, using additional observed data, is needed to improve the prediction accuracy for digestibility.

CRediT authorship contribution statement

Nadeau Elisabet: Writing – review & editing, Investigation, Funding acquisition, Data curation, Conceptualization. **Wallsten Johanna:** Writing – review & editing, Project administration, Methodology, Investigation, Funding acquisition, Data curation, Conceptualization. **Höglind Mats:** Writing – review & editing, Methodology, Conceptualization. **Persson Tomas:** Writing – original draft, Methodology, Funding acquisition, Formal analysis, Data curation, Conceptualization. **Rustas Bengt-Ove:** Writing – review & editing, Project administration, Investigation, Funding acquisition, Data curation, Conceptualization. **Huang Xiao:** Writing – review & editing, Methodology, Conceptualization.

Declaration of Competing Interest

The authors declare that they have no known competing financial interests or personal relationships that could have appeared to influence the work reported in this paper.

Data Availability

Data will be made available on request.

Acknowledgements

This study was funded by the Regional Foundation for Agricultural Research in Northern Sweden (Regional jordbruksforskning för norra Sverige; RJN) (project number 13/2018) and Agroväst. We thank the technical staff at Ås, Lännäs and Röbäcksdalen field research stations for help with field sampling.

References

AHDB, 2018. Barley Growth Guide. Kenilworth, Warwickshire, UK, 39 pp.

Angulo, C., Rötter, R., Lock, R., Enders, A., Fronzek, S., Ewert, F., 2013. Implication of crop model calibration strategies for assessing regional impacts of climate change in Europe. Agric. For. Meteorol. 170, 32–46. https://doi.org/10.1016/j.agrformet.2012.11.017.

Asseng, S., Ewert, F., Rosenzweig, C., Jones, J.W., Hatfield, J.L., Ruane, A.C., Boote, K.J., Thorburn, P.J., Rotter, R.P., Cammarano, D., Brisson, N., Basso, B., Martre, P., Aggarwal, P.K., Angulo, C., Bertuzzi, P., Biernath, C., Challinor, A.J., Doltra, J., Gayler, S., Goldberg, R., Grant, R., Heng, L., Hooker, J., Hunt, L.A., Ingwersen, J., Izaurralde, R.C., Kersebaum, K.C., Muller, C., Naresh Kumar, S., Nendel, C., O/'Leary, G., Olesen, J.E., Osborne, T.M., Palosuo, T., Priesack, E., Ripoche, D., Semenov, M.A., Shcherbak, I., Steduto, P., Stockle, C., Stratonovitch, P., Streck, T., Supit, I., Tao, F., Travasso, M., Waha, K., Wallach, D., White, J.W., Williams, J.R., Wolf, J., 2013. Uncertainty in simulating wheat yields under climate change. Nat. Clim. Change 3, 827–832. https://doi.org/10.1038/nclimate1916.

Asseng, S., Martre, P., Maiorano, A., Rötter, R.P., O'Leary, G.J., Fitzgerald, G.J., Girousse, C., Motzo, R., Giunta, F., Babar, M.A., 2019. Climate change impact and adaptation for wheat protein. Glob. Change Biol. 25, 155–173. https://doi.org/10.1111/gcb.14481.

Banakar, P., Shashank, C., Lakhani, N., 2018. Physically effective fibre in ruminant nutrition: a review. J. Pharmacogn. Phytochem. 7, 303–308.

Bélanger, G., Tremblay, G.F., Mongrain, D., 2008. Yield and nutritive value of the spring growth of an ageing timothy sward. Can. J. Plant Sci. 88, 457–464. https://doi.org/10.4141/CJPS07154.

Bergjord Olsen, A., Persson, T., de Wit, A., Nkurunziza, L., Sindhøj, E., Eckersten, H., 2018. Estimating winter survival of winter wheat by simulations of plant frost tolerance. J. Agron. Crop Sci. 204, 62–73. https://doi.org/10.1111/jac.12238.

Bonesmo, H., Belanger, G., 2002a. Timothy yield and nutritive value by the CATIMO model: I. Growth and nitrogen. Agron. J. 94, 337–345. https://doi.org/10.2134/agronj2002.3370.

Bonesmo, H., Belanger, G., 2002b. Timothy yield and nutritive value by the CATIMO model: II. Digestibility and fiber. Agron. J. 94, 345–350. https://doi.org/10.2134/agronj2002.3450.

Brisson, N., Gary, C., Justes, E., Roche, R., Mary, B., Ripoche, D., Zimmer, D., Sierra, J., Bertuzzi, P., Burger, P., Bussière, F., Cabidoche, Y.M., Cellier, P., Debaeke, P., Gaudillère, J.P., Hénault, C., Maraux, F., Seguin, B., Sinoquet, H., 2003. An overview of the crop model stics. Eur. J. Agron. 18, 309–332. https://doi.org/10.1016/S1161-0301(02)00110-7.

Bueno, A.V.I., Jobim, C.C., Rossi, R.M., Gritti, V.C., Leão, G.F.M., Tres, T.T., 2018. Wilting whole crop black oat with glyphosate for ensiling: effects on nutritive, fermentative, and aerobic stability characteristics. Rev. Bras. De. Zootec. 47 https://doi.org/10.1590/rbz4720170142.

Castro-Montoya, J.M., Dickhoefer, U., 2020. The nutritional value of tropical legume forages fed to ruminants as affected by their growth habit and fed form: A systematic review. Anim. Feed Sci. Technol. 269, 114641 https://doi.org/10.1016/j.anifeedsci.2020.114641.

Challinor, A.J., Wheeler, T., Hemming, D., Upadhyaya, H.D., 2009. Ensemble yield simulations: crop and climate uncertainties, sensitivity to temperature and genotypic adaptation to climate change. Clim. Res. 38, 117–127. https://doi.org/10.3354/cr00779.

Chowdhury, M.R., Wilkinson, R.G., Sinclair, L.A., 2023. Feeding lower-protein diets based on red clover and grass or alfalfa and corn silage does not affect milk production but improves nitrogen use efficiency in dairy cows. J. Dairy Sci. 106, 1773–1789. https://doi.org/10.3168/jds.2022-22607.

Crovetto, G., Galassi, G., Rapetti, L., Sandrucci, A., Tamburini, A., 1998. Effect of the stage of maturity on the nutritive value of whole crop wheat silage. Livest. Prod. Sci. 55, 21–32. https://doi.org/10.1016/S0301-6226(98)00125-0.

Erickson, P.S., Kalscheur, K.F., 2020. Chapter 9 - Nutrition and feeding of dairy cattle. In: Bazer, F.W., Lamb, G.C., Wu, G. (Eds.), Animal Agriculture. Academic Press, pp. 157–180.

Fatima, Z., Ahmed, M., Hussain, M., Abbas, G., Ul-Allah, S., Ahmad, S., Ahmed, N., Ali, M.A., Sarwar, G., Haque, Eu, Iqbal, P., Hussain, S., 2020. The fingerprints of climate warming on cereal crops phenology and adaptation options. Sci. Rep. 10, 18013 https://doi.org/10.1038/s41598-020-74740-3.

Givens, D.I., Humphries, D.J., Kliem, K.E., Kirton, P., Deaville, E.R., 2009. Whole crop cereals: 1. Effect of method of harvest and preservation on chemical composition, apparent digestibility and energy value. Anim. Feed Sci. Technol. 149, 102–113. https://doi.org/10.1016/j.anifeedsci.2008.05.007.

Graux, A.-I., Bellocchi, G., Lardy, R., Soussana, J.-F., 2013. Ensemble modelling of climate change risks and opportunities for managed grasslands in France. Agric. For. Meteorol. 170, 114–131. https://doi.org/10.1016/j.agrformet.2012.06.010.

Gubatz, S., Shewry, P.R., 2010. The development, structure, and composition of the barley grain. In: Ullrich, S.E. (Ed.), Barley: Production, Improvement, and Uses. Wiley-Blackwell Chichester, Sussex, UK, pp. 391–448.

Hansen-Bauer, I., Førland, E.J., Haddeland, I., Hisdal, H., Mayer, S., Nesje, A., Nilsen, J.E. Ø., Sandven, S., Sandø, A.B., Sorteberg, A., Ådlandsvik, B., 2015. Klima i Norge 2100 Kunnskapsgrunnlag for klimatilpasning oppdatert i 2015. NCCS Rep., Oslo 203.

Hao, S., Ryu, D., Western, A., Perry, E., Bogena, H., Franssen, H.J.H., 2021. Performance of a wheat yield prediction model and factors influencing the performance: A review and meta-analysis. Agric. Syst. 194, 103278 https://doi.org/10.1016/j.agsy.2021.103278.

Hetta, M., Mussadiq, Z., Gustavsson, A.-M., Swensson, C., 2012. Effects of hybrid and maturity on performance and nutritive characteristics of forage maize at high latitudes, estimated using the gas production technique. Anim. Feed Sceince Technol. 171, 20–30.

Hochman, Z., Gobbett, D., Holzworth, D., McClelland, T., van Rees, H., Marinoni, O., Garcia, J.N., Horan, H., 2013. Reprint of "Quantifying yield gaps in rainfed cropping systems: a case study of wheat in Australia". Field Crops Res. 143, 65–75. https://doi.org/10.1016/j.fcr.2013.02.001.

Höglind, M., Schapendonk, A., Van Oijen, M., 2001. Timothy growth in Scandinavia: combining quantitative information and simulation modelling. N. Phytol. 151, 355–367. https://doi.org/10.1046/j.0028-646x.2001.00195.x.

Höglind, M., Thorsen, S.M., Semenov, M.A., 2013. Assessing uncertainties in impact of climate change on grass production in Northern Europe using ensembles of global climate models. Agric. For. Meteorol. 170, 103–113. https://doi.org/10.1016/j.agrformet.2012.02.010.

Höglind, M., Van Oijen, M., Cameron, D., Persson, T., 2016. Process-based simulation of growth and overwintering of grassland using the BASGRA model. Ecol. Model. 335, 1–15. https://doi.org/10.1016/j.ecolmodel.2016.04.024.

Höglind, M., Cameron, D., Persson, T., Huang, X., van Oijen, M., 2020. BASGRA_N: A model for grassland productivity, quality and greenhouse gas balance. Ecol. Model. 417, 108925 https://doi.org/10.1016/j.ecolmodel.2019.108925.

Holzworth, D.P., Huth, N.I., deVoil, P.G., Zurcher, E.J., Herrmann, N.I., McLean, G., Chenu, K., van Oosterom, E.J., Snow, V., Murphy, C., 2014. APSIM–evolution towards a new generation of agricultural systems simulation. Environ. Model. Softw. 62, 327–350. https://doi.org/10.1016/j.envsoft.2014.07.009.

Hoogenboom, G., Porter, C., Shelia, V., Boote, K., Singh, U., White, J., Hunt, L., Ogoshi, R., Lizaso, J., Koo, J., 2017. Decision support system for agrotechnology transfer (DSSAT) version 4.7 (https://DSSAT. net). DSSAT Foundation, Gainesville, Florida. USA.

Huuskonen, A., Pesonen, M., Joki-Tokola, E., 2017. Feed intake and live weight gain of Hereford bulls offered diets based on whole-crop barley and whole-crop wheat silages relative to moderately digestible grass silage with or without protein supplementation. Ann. Anim. Sci. 17, 1123. https://doi.org/10.1515/aoas-2017-0007.

IPCC, 2013: Annex II: Climate System Scenario Tables [Prather, M., G. Flato, P. Friedlingstein, C. Jones, J.-F. Lamarque, H. Liao and P. Rasch (eds.)]. In: Climate Change 2013: The Physical Science Basis. Contribution of Working Group I to the Fifth Assessment Report of the Intergovernmental Panel on Climate Change [Stocker, T.F., D. Qin, G.-K. Plattner, M. Tignor, S.K. Allen, J. Boschung, A. Nauels, Y. Xia, V. Bex and P.M. Midgley (eds.)]. Cambridge University Press, Cambridge, United Kingdom and New York, NY, USA.

Jégo, G., Bélanger, G., Tremblay, G.F., Jing, Q., Baron, V.S., 2013. Calibration and performance evaluation of the STICS crop model for simulating timothy growth and nutritive value. Field Crops Res. 151, 65–77. https://doi.org/10.1016/j.fcr.2013.07.003.

Get rights and content

Jones, J.W., Hoogenboom, G., Porter, C.H., Boote, K.J., Batchelor, W.D., Hunt, L.A., Wilkens, P.W., Singh, U., Gijsman, A.J., Ritchie, J.T., 2003. The DSSAT cropping system model. Eur. J. Agron. 18, 235–265. https://doi.org/10.1016/S1161-0301(02)00107-7.

Khorasani, G., Jedel, P., Helm, J., Kennelly, J., 1997. Influence of stage of maturity on yield components and chemical composition of cereal grain silages. Can. J. Anim. Sci. 77, 259–267. https://doi.org/10.4141/A96-034.

Kipling, R.P., Virkajärvi, P., Breitsameter, L., Curnel, Y., De Swaef, T., Gustavsson, A.-M., Hennart, S., Höglind, M., Järvenranta, K., Minet, J., Nendel, C., Persson, T., Picon-Cochard, C., Rolinski, S., Sandars, D.L., Scollan, N.D., Sebek, L., Seddaiu, G., Topp, C. F.E., Twardy, S., Van Middelkoop, J., Wu, L., Bellocchi, G., 2016. Key challenges and priorities for modelling European grasslands under climate change. Sci. Total Environ. 566–567 851–864. https://doi.org/10.1016/j.scitotenv.2016.05.144.

Kolberg, D., Persson, T., Mangerud, K., Riley, H., 2019. Impact of projected climate change on workability, attainable yield, profitability and farm mechanization in Norwegian spring cereals. Soil Tillage Res. 185, 122–138. https://doi.org/10.1016/j.still.2018.09.002.

Korhonen, P., Palosuo, T., Persson, T., Höglind, M., Jégo, G., Van Oijen, M., Gustavsson, A.-M., Bélanger, G., Virkajärvi, P., 2018. Modelling grass yields in northern climates – a comparison of three growth models for timothy. Field Crops Res. 224, 37–47. https://doi.org/10.1016/j.fcr.2018.04.014.

Leão, G.F.M., Jobim, C.C., Neumann, M., Horst, E.H., Santos, S.Kd, Venancio, B.J., Santos, L.C., 2017. Nutritional composition and aerobic stability of winter cereal silage at different storage times. Acta Sci. Anim. Sci. 39, 131–136. https://doi.org/10.4025/actascianimsci.v39i2.34270.

Lehtonen, I., Ruosteenoja, K., Jylhä, K., 2014. Projected changes in European extreme precipitation indices on the basis of global and regional climate model ensembles. Int. J. Climatol. 34, 1208–1222. https://doi.org/10.1002/joc.3758.

Nadeau, E., 2007. Effects of plant species, stage of maturity and additive on the feeding value of whole-crop cereal silage. J. Sci. Food Agric. 87, 789–801. https://doi.org/10.1002/jsfa.2773.

Nadeau, E., Jansson, J., 2010. Vårsådda helsädesgrödor – stråsäd och stråsäd/baljväxt. Försöksrapport 2010 för Mellansvenska försökssamarbetet och Sven. raps 101–103.

Nadeau, E., de Sousa, D.O., Magnusson, A., Hedlund, S., Richardt, W., Nørgaard, P., 2019. Digestibility and protein utilization in wethers fed whole-crop barley or grass silages harvested at different maturity stages, with or without protein supplementation. J. Anim. Sci. 97, 2188–2201. https://doi.org/10.1093/jas/skz076.

Nissinen, O., Kalliainen, P., Jauhiainen, L., 2010. Development of yield and nutritive value of timothy in primary growth and regrowth in northern growing conditions. Agric. Food Sci. 19, 252–268. https://doi.org/10.2137/145960610792912602.

Pan, J., Zhu, Y., Cao, W., 2007. Modeling plant carbon flow and grain starch accumulation in wheat. Field Crops Res. 101, 276–284. https://doi.org/10.1016/j.fcr.2006.12.005.

Park, T.-I., Han, O.-K., Seo, J.-H., Choi, J.-S., Park, K.-H., Kim, J.-G., 2008. New barley cultivars with improved morphological characteristics for whole crop forage in Korea. J. Korean Soc. Grassl. Forage Sci. 28, 193–202. https://doi.org/10.5333/KGFS.2008.28.3.193.

Persson, T., Höglind, M., Gustavsson, A.-M., Halling, M., Jauhiainen, L., Niemeläinen, O., Thorvaldsson, G., Virkajärvi, P., 2014. Evaluation of the LINGRA timothy model under Nordic conditions. Field Crops Res. 161, 87–97. https://doi.org/10.1016/j.fcr.2014.02.012.

Persson, T., Höglind, M., Van Oijen, M., Korhonen, P., Palosuo, T., Jégo, G., Virkajärvi, P., Bélanger, G., Gustavsson, A.M., 2019. Simulation of timothy nutritive value: A comparison of three process-based models. Field Crops Res. 231, 81–92. https://doi.org/10.1016/j.fcr.2018.11.008.

Randby, Å.T., Nadeau, E., Karlsson, L., Johansen, A., 2019. Effect of maturity stage at harvest and kernel processing of whole crop wheat silage on digestibility by dairy cows. Anim. Feed Sci. Technol. 253, 141–152. https://doi.org/10.1016/j.anifeedsci.2019.04.016.

Ritchie, J.T., Godwin, D.C., Otter-Nacke, S., 1985. CERES-Wheat AGRISTARS Publication. Michigan State University, MI, USA, p. 252.

Rodriguez, D., Van Oijen, M., Schapendonk, A.H.C.M., 1999. LINGRA-CC: a sink-source model to simulate the impact of climate change and management on grassland productivity. N. Phytol. 144, 359–368. https://doi.org/10.1046/j.1469-8137.1999.00521.

Rötter, R.P., Palosuo, T., Kersebaum, K.C., Angulo, C., Bindi, M., Ewert, F., Ferrise, R., Hlavinka, P., Moriondo, M., Nendel, C., Olesen, J.E., Patil, R.H., Ruget, F., Takáč, J., Trnka, M., 2012. Simulation of spring barley yield in different climatic zones of Northern and Central Europe: a comparison of nine crop models. Field Crops Res. 133, 23–36. https://doi.org/10.1016/j.fcr.2012.03.016.

Rustas, B.-O., Nørgaard, P., Jalali, A., Nadeau, E., 2010. Effects of physical form and stage of maturity at harvest of whole-crop barley silage on intake, chewing activity, diet selection and faecal particle size of dairy steers. Animal 4, 67–75. https://doi.org/10.1017/S1751731109990887.

Rustas, B.-O., Bertilsson, J., Martinsson, K., Elverstedt, T., Nadeau, E., 2011. Intake and digestion of whole-crop barley and wheat silages by dairy heifers. J. Anim. Sci. 89, 4134–4141. https://doi.org/10.2527/jas.2010-3585.

SAS Institute Inc. 2020. Cary, NC, USA.

Saxton, K.E., Rawls, W.J., 2006. Soil water characteristic estimates by texture and organic matter for hydrologic solutions. Soil Sci. Soc. Am. J. 70, 1569–1578. https://doi.org/10.2136/sssaj2005.0117.

Semenov, M.A., 2008. Simulation of extreme weather events by a stochastic weather generator. Clim. Res. 35, 203–212. https://doi.org/10.3354/cr00731.

Seog, H.-M., Kim, J.-S., Hong, H.-D., Kim, S.-S., Kim, K.-T., 1993. Change in chemical composition of maturing barley kernels. Appl. Biol. Chem. 36, 449–455.

Sivia, D.S., 2006. Data Analysis: A Bayesian Tutorial. Oxford University Press, Oxford, UK.

Slafer, G.A., Molina-Cano, J.L., Savin, R., Araus, J.L., Romagosa, I., 2002. Barley science: recent advances from molecular biology to agronomy of yield and quality. Food Products Press,, Binghamton, NY, USA.

Stöckle, C.O., Kemanian, A.R., Nelson, R.L., Adam, J.C., Sommer, R., Carlson, B., 2014. CropSyst model evolution: From field to regional to global scales and from research to decision support systems. Environ. Model. Softw. 62, 361–369. https://doi.org/10.1016/j.envsoft.2014.09.006.

Tao, F., Yokozawa, M., Liu, J., Zhang, Z., 2008. Climate–crop yield relationships at provincial scales in China and the impacts of recent climate trends. Clim. Res. 38, 83–94. https://doi.org/10.3354/cr00771.

Tao, F., Palosuo, T., Rötter, R.P., Díaz-Ambrona, C.G.H., Mínguez, M.I., Semenov, M.A., Kersebaum, K.C., Cammarano, D., Specka, X., Nendel, C., 2020. Why do crop models diverge substantially in climate impact projections? a comprehensive analysis based on eight barley crop models. Agric. For. Meteorol. 281, 107851 https://doi.org/10.1016/j.agrformet.2019.107851.

Tripathi, A., Tripathi, D.K., Chauhan, D., Kumar, N., Singh, G., 2016. Paradigms of climate change impacts on some major food sources of the world: a review on current knowledge and future prospects. Agric., Ecosyst. Environ. 216, 356–373. https://doi.org/10.1016/j.agee.2015.09.034.

Van Oijen, M., Rougier, J., Smith, R., 2005. Bayesian calibration of process-based forest models: bridging the gap between models and data. Tree Physiol. 25, 915–927. https://doi.org/10.1093/treephys/25.7.915.

Wallsten, J., Hatfield, R., 2016. Cell wall chemical characteristics of whole-crop cereal silages harvested at three maturity stages. J. Sci. Food Agric. 96, 3604–3612. https://doi.org/10.1002/jsfa.7736.

Wallsten, J., Nadeau, E., Bertilsson, J., Martinsson, K., 2009. Voluntary intake and diet selection by dairy heifers fed ensiled whole-crop barley and oats harvested at different stages of maturity. Livest. Sci. 122, 94–98. https://doi.org/10.1016/j.livsci.2008.07.031.

Wallsten, J., Bertilsson, J., Nadeau, E., Martinsson, K., 2010. Digestibility of whole-crop barley and oat silages in dairy heifers. Animal 4, 432–438. https://doi.org/10.1017/S1751731109991212.

Wang, J., Vanga, S.K., Saxena, R., Orsat, V., Raghavan, V., 2018. Effect of climate change on the yield of cereal crops: a review. Climate 6, 41. https://doi.org/10.3390/cli6020041.

Wilkinson, J.M., 2011. Re-defining efficiency of feed use by livestock. Animal 5, 1014–1022. https://doi.org/10.1017/S175173111100005X.

Willmott, C.J., 1982. Some comments on the evaluation of model performace. Bull. Am. Meteorol. Soc. 63, 1309–1313.

Xu, L., Xu, Z., Chen, M., Zhang, J., 2021. Effects of seeding rate, fertilizing time and fertilizer type on yield, nutritive value and silage quality of whole-crop wheat. Trop. Grassl. -Forrajes Trop. 9, 225–234. https://doi.org/10.17138/tgft(9)225-234.

Zadoks, J.C., Chang, T.T., Konzak, C.F., 1974. A decimal code for the growth stages of cereals. Weed Res. 14, 415–421.